Available online at www.sciencedirect.com
SCIENCE DIRECT
Journal of Photochemistry and Photobiology A: Chemistry 175 (2005) 108–117
Journal of Photochemistry and Photobiology A:Chemistry
www.elsevier.com/locate/jphotochem

Modified push–pull expanded corroles: Syntheses, structure and nonlinear optical properties

Rajneesh Misra [a], Rajeev Kumar [a], Viswanathan PrabhuRaja [a], Tavarekere K. Chandrashekar [a,b,*]

[a] *Department of Chemistry, Indian Institute of Technology, Kanpur, UP 208016, India*
[b] *Regional Research Laboratory, Trivandrum, Kerala 695019, India*

Received 15 February 2005; received in revised form 27 March 2005; accepted 17 April 2005
Available online 31 May 2005

Abstract

A series of expanded corroles containing electron donating and electron withdrawing groups on the opposite *meso*-phenyl groups have been synthesized through a simple [3 + 2] oxidative coupling reaction of a tripyrrane containing electron donating group (–OMe, –Me) and dipyrromethane containing an electron withdrawing group (–NO_2, –CN) in moderate yields. The photophysical studies reveal decrease in singlet lifetimes and quantum yields relative to normal corrole. The quantum yield, lifetime and Stokes shift depend on the nature of solvent and the largest Stokes shifts are observed in the polar solvents, suggesting a polar nature of the excited state. The molecular first hyperpolarizability (β) measured for expanded corroles shows moderate values (24–30 $\times$ 10^{-30} esu). These values are approximately 5–6 times larger than those observed for structurally similar 18 π substituted tetraphenyl porphyrins, revealing that the nonlinear optical (NLO) response can be increased by increasing the number of π electrons in conjugation. An attempt has been made to correlate the observed β values with structure of the molecule and orientation of donor acceptor groups. The single crystal X-ray structure of **13** and **14** reveals nonplanarity of macrocycle and the dihedral angles between the macrocyclic π system and the *meso*-aryl rings vary in the range of (33–75°) preventing an effective charge transfer interaction between the donor and acceptor groups required for observation of large β value. Formation of supramolecular ladder type structure for compound **13** through noncovalent C–H···O hydrogen bonding interactions is also described.
© 2005 Elsevier B.V. All rights reserved.

Keywords: Expanded corrole; Nonlinear optics; Oxidative coupling reaction; Push–pull porphyrinoids; Supramolecular chemistry

1. Introduction

Organic molecules containing conjugated π electrons linked to electron donor (D) at one end and electron acceptor (A) at the opposite end have been recognized as one class of nonlinear optical materials for potential application in optical communication and information storage devices [1]. Such D–π–A systems are expected to exhibit a large charge asymmetry and hence, show large second order nonlinearity (β) [2]. Recently several D–π–A systems based on porphyrin molecules have been constructed and their nonlinear optical behavior have been documented in literature [3]. Specifically electron donating groups, such as –NMe_2, –NH_2 and electron withdrawing groups, such as –NO_2, –CHO, –F are substituted on the periphery of the porphyrin molecules and their second order nonlinear optical behavior have been studied. In general such systems are known as push–pull porphyrins. The observed β values depend on the nature of the porphyrin, its substituents and the nature of linker groups. The molecular structures of few such D–π–A systems **1**–**6** are shown in Fig. 1.

Recently we have reported the synthesis of an expanded corrole bearing a *meso*-ferrocenyl [4] substituent **7** and have measured their nonlinear optical response by Z-scan method. It has been shown that there is an electronic communication between the expanded corrole skeleton and the *meso*-substituted ferrocenyl moiety. In continuation of this work,

* Corresponding author. Tel.: +91 471 2515333; fax: +91 471 2491712.
E-mail address: tkc@iitk.ac.in (T.K. Chandrashekar).

1010-6030/$ – see front matter © 2005 Elsevier B.V. All rights reserved.
doi:10.1016/j.jphotochem.2005.04.024

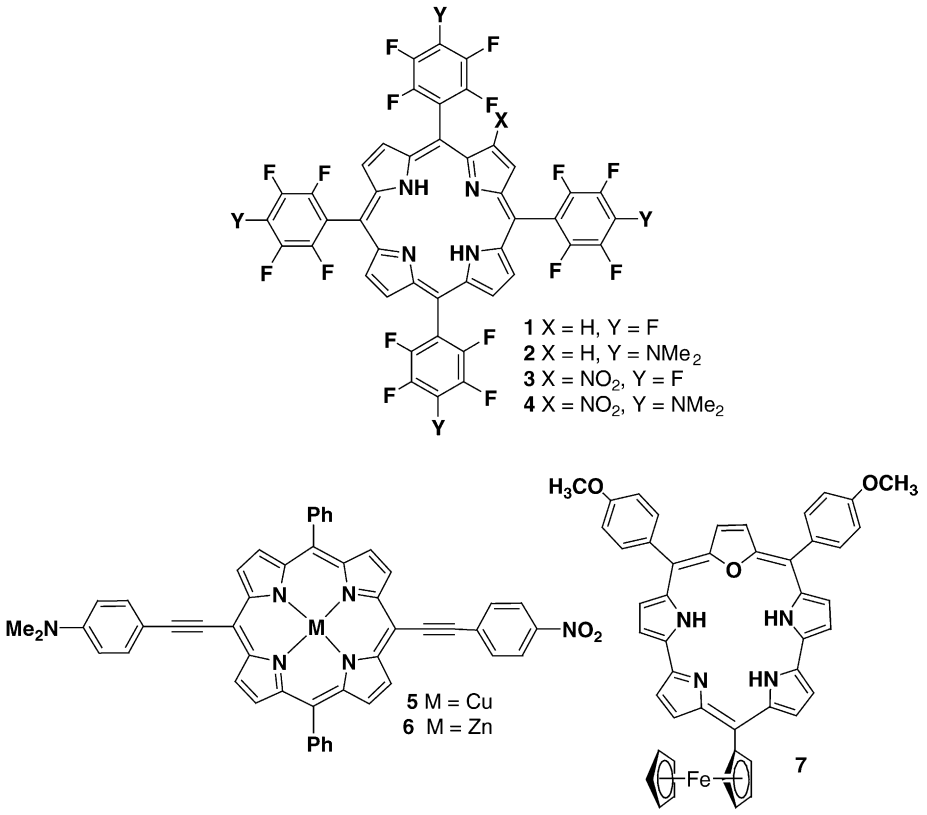

Fig. 1. Molecular structure of push–pull porphyrins and expanded corroles.

in this paper we describe the synthesis of four new types of push–pull expanded corroles and studied their photophysical properties and second order nonlinear optical response by Hyper–Rayleigh scattering (HRS) method. Single crystal X-ray structures of two push–pull expanded corroles have also been reported. The new expanded corroles show moderate β values in the range ($24–30 \times 10^{-30}$ esu) which are slightly larger than the traditional push–pull porphyrins [3b]. However, these β values are much lower than the value observed for push–pull porphyrins linked by ethynyl spacer [3c] groups. An attempt has been made to rationalize the observed β values in terms of the molecular structure and the orientation of the donor, acceptor groups.

2. Experimental

2.1. Instrumentation

Electronic spectra were recorded on Perkin-Elmer Lambda 20 UV–vis spectrophotometer. The fluorescence spectra were recorded on a SPEX-Fluorolog F112X spectrofluorimeter. Fluorescence lifetime was measured on a IBH picosecond single photon counting system using a 440 nm IBH NanoLED source and Hamamatsu C4878-02 MCP detector. The fluorescence decay profiles were deconvoluted using IBH data station software V2.1, fitted with mono or biexponential decay. Proton NMR spectra were obtained on a 400 MHz JEOL spectrometer in $CDCl_3$. FAB-MS spectra were obtained on a JEOL-SX-120/DA6000 spectrometer. The dipole moment of expanded corroles was calculated by TITAN software using Hartree–Fock, 3-21G basis set.

2.2. Crystallography

X-ray data were collected at 100 K on Enraf Nonius MACH2 diffractometer, equipped with graphite monochromated $Mo_{K\alpha}$ radiation ($\lambda = 0.71073$ Å). Lorentz and polarization corrections were applied for all compounds. A semi empirical absorption correction was carried out. The crystal structure of all the compounds were solved by direct methods, as included in SHELXTL program package [5a]. Missing atoms were located in subsequent difference Fourier maps and included in the refinement. The structures of all compounds were refined by full-matrix least squares refinement on F^2 (SHELXL-97) [5b]. Hydrogen atoms were placed geometrically and refined using a riding model, including free rotation about C–C bonds for methyl groups with U_{iso} constrained at 1.2 for non-methyl groups, and 1.5 for methyl groups times U_{eq} of the carrier carbon atom. All non hydrogen atoms were refined anisotropically.

CCDC–255314 (for **13**) and CCDC–255315 (for **14**) contain the supplementary crystallographic data for this paper. These data can be obtained free of charge via www.ccdc.cam.

ac.uk/conts/retrieving.html (or from the Cambridge Crystallographic Centre, 12 union Road, Cambridge CB21 EZ, UK; Fax: (+44) 1223-336-033; or deposit@ccdc.cam.ac.uk).

2.3. Hyper–Rayleigh scattering measurements

First hyperpolarizability of all the molecules was determined by HRS technique using external reference method. Experiments were carried out in dichloromethane employing a fundamental wavelength (1064 nm) of a Q-switched Nd:YAG laser (Lab 170, Spectra Physics, 10 HZ, 8 ns). All the data were collected at laser powers 17–20 mJ/pulse. The experimental set-up used for the HRS measurements is similar to previous description [6]. In brief, the exciting beam is focused by a biconvex lens (f.l.8 cm) to a spot 5-cm away after passing through the cylindrical glass cell containing the sample. A visible photomultiplier tube (PMT) collects scattered light in the perpendicular direction. A high through-put monochromator (Jobin Yvon, TRIAX 550) was used for wavelength dispersion and no other collection optics was employed. The monochromator was scanned and at each wavelength, the signal output from the PMT was averaged over 256 laser shots. The input power was monitored using a power meter. The intensity of the second harmonic scattered light, $I_{2\omega}$ (taken from peak of Lorentzian fit) for a two component mixture of solvent and solute is given by

$$I_{2\omega} = G\{N_{\text{solvent}}\,\beta^2_{\text{solvent}} + N_{\text{solute}}\,\beta^2_{\text{solute}}\}I^2_{\omega}$$

The quadratic coefficient $I_{2\omega}/I^2_{\omega}$ varies linearly with number density, N_{solute} of the solute, if β and N for the solvent are fixed. HRS measurements were carried for all compounds in the concentration range varying from 10^{-5} to 10^{-6} M. Since low concentrations of solute were used, we assume that the presence of the solute molecules does not change the number density of the solvent molecules, N_{solvent} significantly. First the β value of *para*-nitroaniline (pNA) was studied as 18.7×10^{-30} esu in chloroform by external reference method [7] using pNA in dioxane as the reference.

2.4. Chemicals

All NMR solvents were used as received. Solvents like dichloromethane, tetrahydrofuran and *n*-hexane were purified and distilled by standard procedure. Furan-dialcohol and tripyrranes were synthesized according to published procedure and stored under inert atmosphere.

2.5. Syntheses

2.5.1. 5-(4-Nitrophenyl)dipyrromethane (**8**)

A mixture of pyrrole (4.58 ml, 66 mmol) and 4-nitrobenzaldehyde (0.4 g, 2.6 mmol) was degassed by bubbling argon for 10 min. Trifluoroacetic acid (0.02 ml, 0.26 mmol) was added, the mixture was stirred at room temperature for 20 min. It was diluted with CH_2Cl_2 (50 ml) and then washed with 0.1 M NaOH. The organic layer was dried over anhydrous sodium sulfate. The solvent was removed under reduced pressure and the unreacted pyrrole was removed by vacuum distillation at room temperature. The resulting viscous liquid was purified by column chromatography (silica gel (100–200 mesh), ethyl acetate/petroleum ether (15/85)), evaporation gave **8** as a pale yellow solid. Yield 78%; FAB-MS: *m*/*z* (%): 267 (85) [M^+]; ^{1}H NMR (400 MHz, $CDCl_3$, 25 °C): δ = 5.510 (s, 1H), 5.80 (m, 2H), 6.10 (q, 2H), 6.67 (m, 2H), 7.37 (d, 2H), 7.92 (br s, 2H), 8.10 (d, 2H); elemental analysis: calcd (%) for $C_{15}H_{13}N_3O_2$: C 67.41, H 4.87, N 15.73; found: C 67.72, H 4.97, N 15.43.

2.5.2. 5-(4-Cyanophenyl)dipyrromethane (**9**)

A mixture of pyrrole (6.6 ml, 95.3 mmol) and 4-cyanobenzaldehyde (0.5 g, 3.81 mmol) was degassed by bubbling argon for 10 min. Trifluoroacetic acid (0.03 ml, 0.38 mmol) was added, the mixture was stirred at room temperature for 20 min. It was diluted with CH_2Cl_2 (50 ml) and then washed with 0.1 M NaOH. The organic layer was dried over anhydrous sodium sulfate. The solvent was removed under reduced pressure and the unreacted pyrrole was removed by vacuum distillation at room temperature. The resulting viscous liquid was purified by column chromatography (silica gel (100–200 mesh), ethyl acetate/petroleum ether (20/80), evaporation gave **9** as a white solid. Yield 48%; FAB-MS: *m*/*z* (%): 247 (100) [M^+]; ^{1}H NMR (400 MHz, $CDCl_3$, 25 °C): δ = 5.46 (s, 1H), 5.78 (m, 2H), 6.10 (q, 2H), 6.68 (m, 2H), 7.25 (d, 2H), 7.54 (d, 2H), 7.91 (br s, 2H); elemental analysis: calcd (%) for $C_{16}H_{13}N_3$: C 77.73, H 5.30, N 17.01; found: C 77.52, H 5.42, N 17.04.

2.5.3. 5,10-(4-Methoxyphenyl)-19-(4-nitrophenyl)-25-oxasmaragdyrin (**12**)

The oxatripyrrane **10** (0.530 g, 1.120 mmol) and 5-(4-nitrophenyl)dipyrromethane **8** (0.319 g, 1.120 mmol) were dissolved in dry dichloromethane (250 ml) and stirred under nitrogen atmosphere for 5 min. TFA (0.093 ml, 0.120 mmol) was added and the stirring was continued for further 90 min. Chloranil (0.88 g, 3.6 mmol) was added and the reaction mixture was exposed to air and refluxed for a further 90 min. The solvent was evaporated in vacuum. The residue was purified by chromatography on a basic alumina column, second green band which eluted with dichloromethane gave **12** in (0.32 g, 38%), which decomposes above 300 °C.

The above procedure was followed by using the respective oxatripyrranes **10**, **11** with dipyrromethane **8**, **9** to obtain other push–pull expanded corroles.

12; FAB-MS: *m*/*z* (%): 698 (50) [M^+]; ^{1}H NMR (400 MHz, $CDCl_3$, 25 °C, TMS): δ = 9.57 (d, J = 4.4 Hz, 2H), 9.48 (d, J = 4.4 Hz, 2H), 8.92 (d, J = 4.4 Hz, 2H), 8.86 (s, 2H), 8.55 (d, J = 4.4 Hz, 2H), 8.67 (d, J = 8.4 Hz, 2H), 8.52 (d, J = 8.4 Hz, 2H), 8.10 (d, J = 8.4 Hz, 4H), 7.31 (d, J = 8.4 Hz, 4H), 4.07 (s, 6H); UV–vis (CH_2Cl_2): λ_{max} ($\varepsilon \times 10^{-4}$ M^{-1} cm^{-1}); 443

(17.3), 457 (sh, 16.2), 559 (1.54), 603 (1.38), 649 (1.09), 717 (1.96); (CH_2Cl_2/TFA): λ_{max} ($\varepsilon \times 10^{-4}\,M^{-1}\,cm^{-1}$): 455 (17.23), 486 (sh, 12.51), 614 (1.35), 672 (2.08), 739 (5.39): elemental analysis: calcd (%) for $C_{43}H_{31}N_5O_5$: C 74.03, H 4.44, N 10.03; found: C 74.09, H 4.39, N 9.98.

*2.5.4. **13**; FAB-MS: m/z (%): 666 (45) [M⁺]; ^{1}H NMR (400 MHz, CDCl₃, 25 °C, TMS)*

δ = 9.56 (d, J = 4.4 Hz, 2H), 9.46 (d, J = 4.4 Hz, 2H), 8.88 (d, J = 4.4 Hz, 2H), 8.84 (s, 2H), 8.53 (d, J = 4.4 Hz, 2H), 8.67 (d, J = 11.2 Hz, 2H), 8.52 (d, J = 11.2 Hz, 2H), 8.05 (d, J = 7.8 Hz, 4H), 7.56 (d, J = 7.8 Hz, 4H), 2.67 (s, 6H); UV–vis (CH_2Cl_2): λ_{max} ($\varepsilon \times 10^{-4}\,M^{-1}\,cm^{-1}$); 443 (14.10), 456 (sh, 13.3), 558 (1.2), 602 (1.22), 648 (1.00), 717 (1.84); (CH_2Cl_2/TFA): λ_{max} ($\varepsilon \times 10^{-4}\,M^{-1}\,cm^{-1}$): 452 (15.06), 485 (sh, 11.05), 667 (1.91), 737 (4.70): elemental analysis: calcd (%) for $C_{43}H_{31}N_5O_3$: C 77.58, H 4.69, N 10.52; found: C 77.63, H 77.64, N 10.55.

*2.5.5. **14**; FAB-MS: m/z (%): 678 (45) [M⁺]; ^{1}H NMR (400 MHz, CDCl₃, 25 °C, TMS)*

δ = 9.54 (d, J = 4.4 Hz, 2H), 9.42 (d, J = 4.4 Hz, 2H), 8.85 (d, J = 4.4 Hz, 2H), 8.80 (s, 2H), 8.53 (d, J = 4.4 Hz, 2H), 8.45 (d, J = 7.8 Hz, 2H), 8.08 (d, J = 7.8 Hz, 2H), 8.06 (d, J = 8.4 Hz, 4H), 7.30 (d, J = 8.4 Hz, 4H), 4.07 (s, 6H); UV–vis (CH_2Cl_2): λ_{max} ($\varepsilon \times 10^{-4}\,M^{-1}\,cm^{-1}$); 452 (19.2), 486 (sh, 4.6), 558 (1.13), 602 (1.2), 650 (1.10), 725 (2.07); (CH_2Cl_2/TFA); λ_{max} ($\varepsilon \times 10^{-4}\,M^{-1}\,cm^{-1}$): 454 (21.3), 487 (9.13), 670 (1.73), 731 (4.13): elemental analysis: calcd (%) for $C_{44}H_{31}N_5O_3$: C 77.97, H 4.61, N 10.33; found: C 78.01, H 4.59, N 10.31.

*2.5.6. **15**; FAB-MS: m/z (%): 646 (95) [M⁺]; ^{1}H NMR (400 MHz, CDCl₃, 25 °C, TMS)*

δ = 9.52 (d, J = 4.2 Hz, 2H), 9.42 (d, J = 4.2 Hz, 2H), 8.86 (d, J = 4.2 Hz, 2H), 8.81 (s, 2H), 8.50 (d, J = 4.2 Hz, 2H), 8.45 (d, J = 7.8 Hz, 2H), 8.08 (d, J = 7.8 Hz, 2H), 8.04 (d, J = 7.5 Hz, 4H), 7.56 (d, J = 7.5 Hz, 4H), 2.67 (s, 6H); UV–vis (CH_2Cl_2): λ_{max} ($\varepsilon \times 10^{-4}\,M^{-1}\,cm^{-1}$); 450 (17.83), 557 (1.42), 598 (1.34), 648 (1.28), 717 (1.79); (CH_2Cl_2/TFA): λ_{max} ($\varepsilon \times 10^{-4}\,M^{-1}\,cm^{-1}$): 453 (20.59), 485 (sh, 9.19), 663 (2.00), 727 (4.09): elemental analysis: calcd (%) for $C_{44}H_{31}N_5O$: C 81.84, H 4.84, N 10.84; found: C 81.43, H 4.84, N 10.91.

3. Results and discussion

The push–pull expanded corroles were synthesized by oxidative coupling reaction of an oxa-tripyrromethane containing an electron donating group and a dipyrromethane containing an electron withdrawing substituent. The dipyrromethanes **8** and **9** were synthesized by condensing 4-nitrobenzaldehyde and 4-cyanobenzaldehyde with pyrrole in presence of 0.1 eq. of trifluoroacetic acid in good yields (Scheme 1a). Both **8** and **9** were found to be stable and can be stored in the freezer for months. The oxatripyrromethanes **10** and **11** were synthesized by our pervious method [8], by the reaction of furan-dialcohol and pyrrole. The acid catalysed [3 + 2] oxidative coupling reaction of the dipyrromethane and tripyrromethane followed by chloranil oxidation (Scheme 1b) gave the expected push–pull expanded corroles **12**–**15** as a major product in ≈42% yield. Trace amount

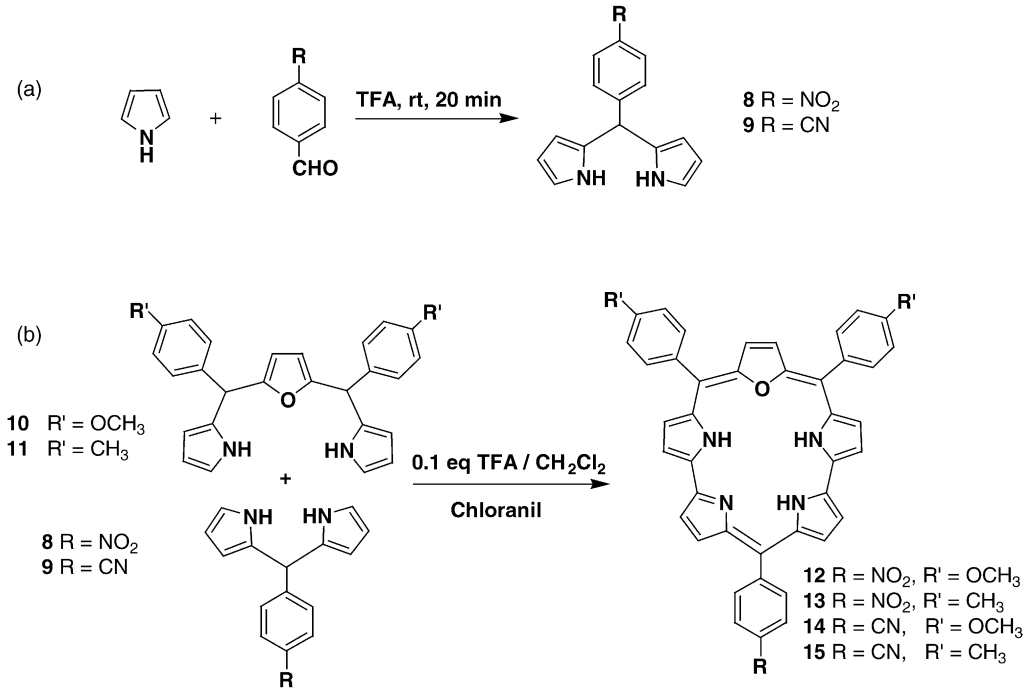

Scheme 1. (a) Syntheses of **8**–**9** and (b) syntheses of **12**–**15**.

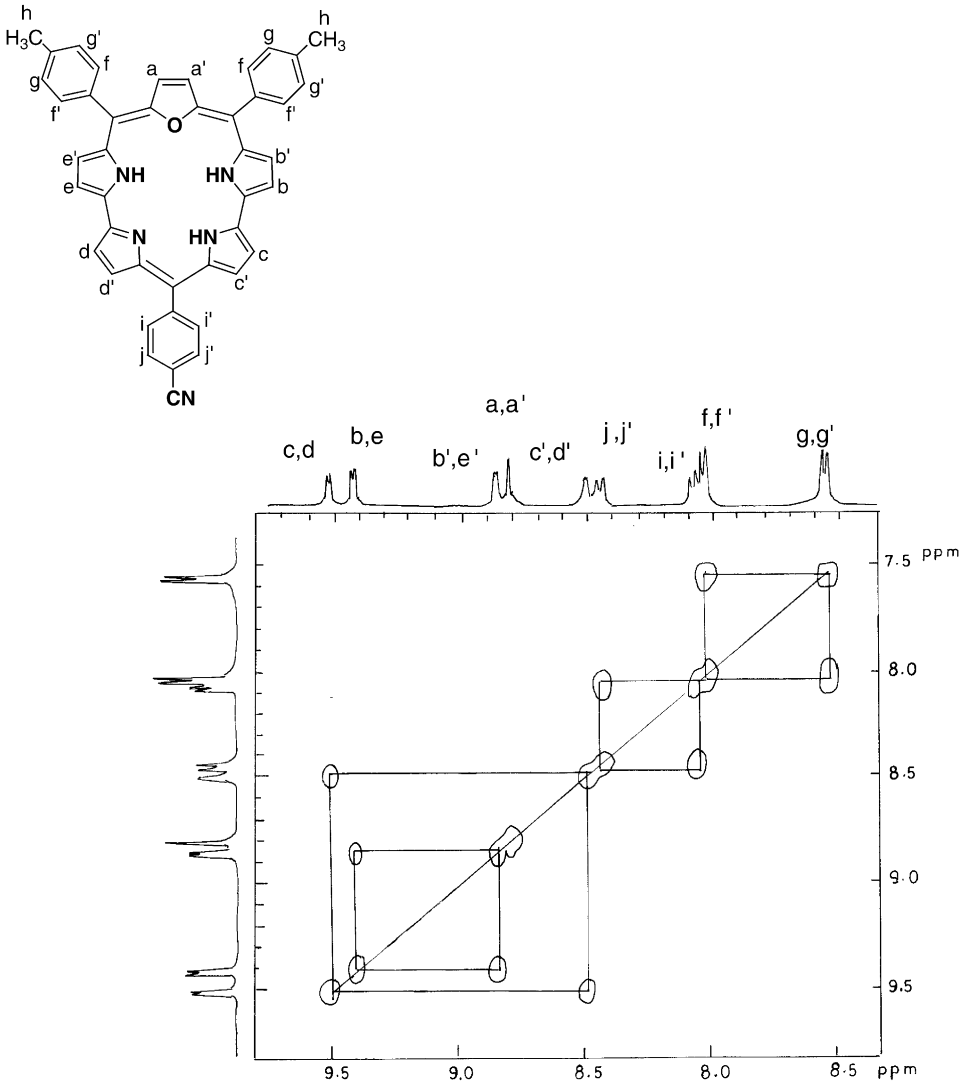

Fig. 2. ^{1}H–^{1}H COSY spectrum of **15** in $CDCl_3$ at room temperature. The observed correlations are marked.

of the monooxa porphyrin [9] and rubyrin [10] were also formed as side products. The desired product was separated by column chromatography using CH_2Cl_2 as the solvent. Compound **12**–**15** were found to be stable in solid and solution phase. The FAB-mass spectra and the CHN analysis confirmed their composition.

A detailed analysis of ^{1}H and 2D NMR spectra of **12**–**15** confirms the proposed solution structures. A typical ^{1}H and ^{1}H–^{1}H COSY spectra observed for **15** is depicted (Fig. 2) and the assignments are marked. The bipyrrole protons (b, b′; c, c′; d, d′; e, e′) resonate as four well resolved doublets in the δ = 8–10 ppm region. The outer bipyrrole protons (b′, e′; c′, d′) are more shielded as compared to inner bipyrrole protons (b, e; c, d) because of upfield ring current contribution of the *meso*-aryl ring. The β-CH protons of the furan ring (a, a′) appear as a sharp singlet at δ = 8.81 ppm. There are two sets of protons for *meso*-tolyl group, the protons present next to carbon atom connected to *meso*-position (f, f′) resonate at δ = 8.04 ppm and the other two protons (g, g′) resonate at δ = 7.55 ppm. The 4-cyanophenyl group also have two sets of protons, the protons present next to carbon atom connected to *meso*-position (i, i′) resonate at δ = 8.07 ppm and the other two protons (j, j′) resonate at δ = 8.45 ppm. The methyl protons resonate at δ = 2.7 ppm. The equivalence of bipyrrole protons (b′, e′; b, e; c, d; c′, d′) in the ^{1}H NMR spectrum suggests that the three –NH protons exchange sites between four bipyrrole nitrogen centers, indicating that the molecule adopts a symmetric conformation in solution with respect to the mirror plane passing through the furan oxygen atom and the opposite methane bridge, suggesting a rapid tautomerism between inner N–H protons, consistent with our earlier observation on oxa-expanded corroles [4].

3.1. Absorption and emission properties

The electronic absorption spectra of **12**–**15** show typical intense Soret like band in the region 440–455 nm and four Q bands in the region 550–750 nm, suggesting the porphyrinic

Table 1
Photophysical data of expanded corroles in different solvents at 300 K

Compound	Solvent	λ_{abs} (nm)	λ_{em} (nm)	Stokes shift (cm^{-1})	ϕ_f	τ (ns)	k_f ($10^8\ s^{-1}$)	k_{nr} ($10^8\ s^{-1}$)
12	Benzene	448	739	8789	0.080	4.20	0.19	2.18
	Toluene	448	739	8789	0.075	4.33	0.17	2.13
	THF	446	761	9280	0.013	0.66	0.19	14.80
13	Benzene	448	737	8752	0.098	4.58	0.21	1.96
	Toluene	448	737	8752	0.083	4.68	0.17	1.95
	THF	445	758	9279	0.018	0.87	0.21	11.20
14	Benzene	453	724	8262	0.147	4.88	0.30	1.74
	Toluene	453	724	8262	0.141	5.65	0.24	1.52
	THF	452	736	8536	0.072	5.60	0.13	1.65
15	Benzene	452	722	8273	0.175	5.94	0.29	1.38
	Toluene	452	722	8273	0.166	4.39	0.37	1.89
	THF	451	730	8474	0.179	5.26	0.34	1.55

nature of macrocycles [11]. The red shift observed with respect to normal tetraphenyl porphyrin (18 π) indicates the effect of extended π conjugation in push–pull expanded corrole (22 π). The monoprotonation leads to red shift (5–8 nm) in both Soret and Q bands relative to free base form is consistent with the *meso*-aryl nature of corroles. In compounds **12** and **13** bearing *para*-nitro group Soret band is slightly split while in compounds **14** and **15** bearing *para*-cyano group sharp Soret band is observed, suggesting slight asymmetry of the macrocycle due to a possible rotation of the nitro group [12] attached to the *meso*-phenyl ring. This in turn can perturb the electronic states resulting in the split Soret band. Furthermore the absorption maxima were found to be dependent on solvent polarity and small shifts were observed in different solvents.

The emission spectra for compounds **12**–**15** were recorded in various solvents and emission parameters calculated are tabulated in Table 1. Emission spectra of **12**–**15** in toluene are shown in Fig. 3a and corresponding decay for compound **12** is shown in Fig. 3b. The quantum yields were calculated using tetraphenyl porphyrin as the reference compound ($\phi = 0.11$) and the lifetime data was fitted satisfactorily to a mono exponential curve with good χ^2 values (1.03–1.10), in most cases. However, in a couple of cases the decay curves better fitted for biexponential expression. The radiative (k_f) and non-radiative (k_{nr}) decay were obtained by following expressions:

$$k_f = \frac{\phi_f}{\tau}$$

$$k_{nr} = \frac{1 - \phi_f}{\tau}$$

Inspection of the Table 1 reveals following observations: (a) regular emission band shifts to lower energies upon increasing the solvent polarity. (b) The quantum yield for nitro derivatives is lower than cyano derivatives and a decrease in quantum yield is observed upon increase in polarity of solvent with exception of **15**. (c) The singlet lifetimes for **12**–**15** are slightly lower relative to that of monoxa corrole (6.04 ns) [13]. (d) The magnitude of Stokes shift increases with increasing solvent polarity. The shift to the lower energies upon increasing solvent polarity suggests excited state must be polar in nature and progressively stabilized in more polar solvents [12]. The large Stokes shift observed in polar solvents also justify such a conclusion. The decrease in quantum yield for nitro derivatives relative to cyano deriva-

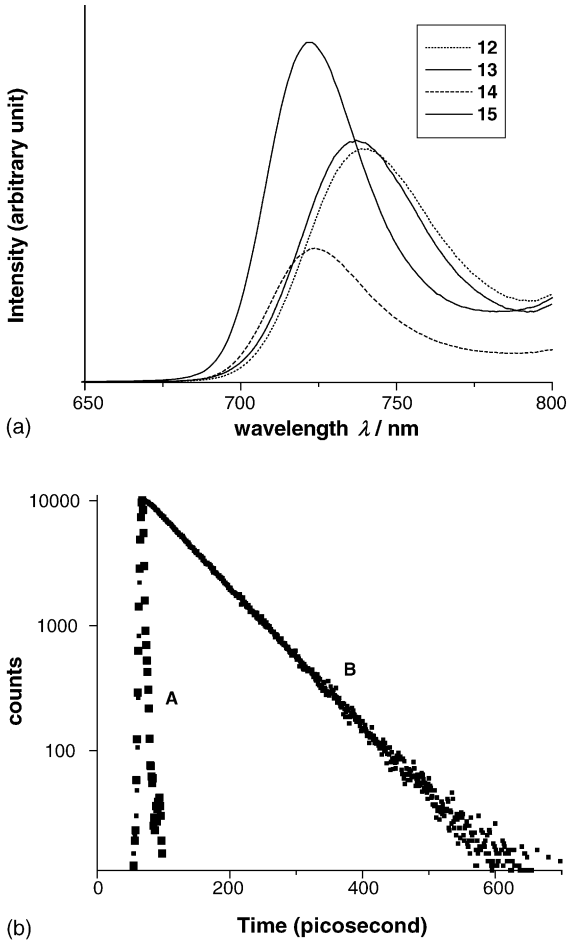

Fig. 3. (a) Fluorescence spectra of compounds **12**–**15** in toluene at 300 K ($\lambda_{ex} = 447$ nm). (b) Time-resolved fluorescence decay curve A shows the instrument response function B shows compound **12** in toluene.

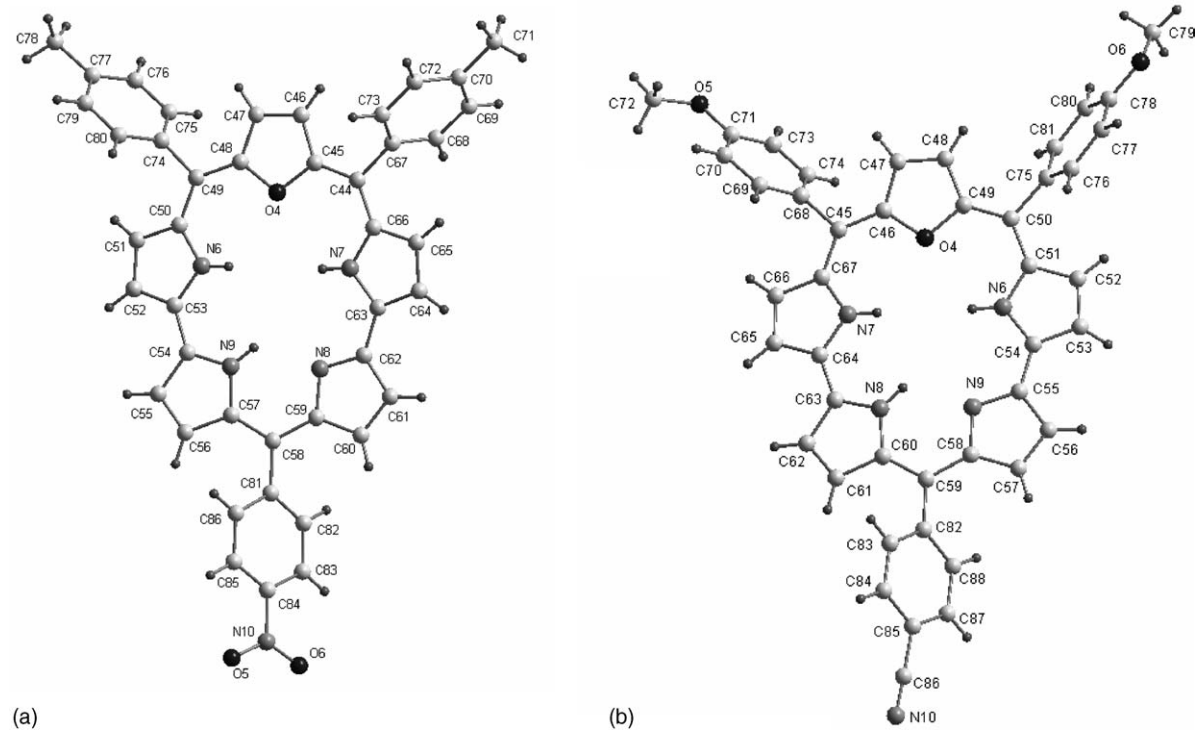

Fig. 4. Single crystal X-ray structures (top view) (a) **13** and (b) **14**.

tive suggests the predominance of nonradiative deactivation dynamics in ground state. In general it has been shown that the fluorescence of aromatic substances containing nitro group is generally weak, primarily as a result of large values of k_{nr} [14]. In the present study it has been observed that the k_{nr} values are about 1.5–7 times larger for expanded corroles **12** and **13**. The large k_{nr} values observed in THF for compound **12** and **13** is consistent with the polar nature of excited state. The larger quantum yield for **14** and **15** is consistent with the larger radiative k_f decay values at the expense of nonradiative k_{nr} decay values [15]. A small decrease observed in the life time for **12**–**15** relative to mono-oxacorrole suggests that the rate of intersystem crossing and internal conversion are predominant in push–pull expanded corroles, relative to mono-oxacorrole [14].

3.2. Crystallographic characterization

The proposed structure of the push–pull expanded corroles is further confirmed by solving single crystal X-ray structure for **13** and **14** and the structures are depicted in Fig. 4. In both the cases there are two crystallographically independent molecules in the unit cell and the bond lengths and bond angles are slightly different. The structure reveals nonplanarity of expanded corrole framework, which is mainly due to the strain imposed by the introduction of direct pyrrole–pyrrole link, which reduces the cavity size relative to the normal sapphyrin [16] molecule. The important crystallographic parameters are listed in Table 2. The reduced cavity size causes the steric repulsion between the three imino pyrrole nitrogens adding to the nonplanarity of macrocycle. The aromatic nature of the macrocycle is evident from the observation that the C_β–C_β distances are shorter than the corresponding C_α–C_β distance [11] (for example, in **13** C_β–C_β furan 1.352, C_α–C_β 1.417; C_β–C_β pyrrole 1.387, C_α–C_β 1.403 Å).

The dihedral angle between the expanded corrole plane defined by three *meso*-carbons and the plane containing *meso*-aryl substituents and the C–C bond length linking the aryl group to *meso*-carbons are dependent on the nature of donor acceptor group present on *meso*-aryl ring. This data are tabulated in Table 3. The important observation in the bond length data is the significant reduction (0.2 Å) in the C–C bond length linking the *meso*-carbon and the phenyl ring for the *meso*-aryl group containing the electron acceptor nitro and cyano group for **13** and **14**, respectively, relative to the C–C bond lengths of the phenyl rings containing electron donor groups, implying more olefinic character of C–C bond. The large dihedral angle observed clearly suggests absence of any effective π overlap between the π system of macrocycle and *meso*-aryl group.

Another important observation in the crystal structure of **13** is formation of ladder type supramolecular assembly shown in Fig. 5, formed by three weak intermolecular C–H···O interactions. Specifically the nitro oxygen of one of the crystallographically independent molecule (shown in purple color) forms a C–H···O hydrogen bond (shown in blue color) with the C–H of *meso*-aryl group of neighbouring molecule leading to one dimension linear array

Table 2
Crystallographic data for expanded corrole **13** and **14**

Crystallographic data	**13**	**14**
Solvent of crystallization	CH_2Cl_2/hexane	CH_2Cl_2
Empirical formula	$C_{87}H_{64}Cl_2N_{10}O_6$	$C_{88}H_{62}N_{10}O_6$
T (K)	100	100
Crystal system	Triclinic	Monoclinic
Space group	P-1	P2(1)/n
V (Å^3)	3451.1	6583
a (Å^3)	11.753	9.954
b (Å^3)	16.076	17.976
c (Å^3)	20.998	36.816
α (°)	111.62	90
β (°)	92.78	92.20
γ (°)	107.88	90
Z	2	4
ρ_{calcd} (Mg m^{-3})	1.315	1.368
Measured reflections	23324	43626
Unique reflections	16470	16302
R (in)	0.0332	0.1086
F(0 0 0)	1426	2832
Limiting indices	$-15 \le h \le 15$, $-19 \le k \le 21$, $-27 \le l \le 28$	$-13 \le h \le 7$, $-23 \le k \le 23$, $-49 \le l \le 48$
GoF (F^2)	1.030	1.087
Final R indices [$I > 2\sigma(I)$]		
$R1$	0.0906	0.1049
$wR2$	0.2133	0.1801
R indices (all data)		
$R1$	0.1271	0.1836
$wR2$	0.2375	0.2084

Table 3
Important bond lengths and dihedral angles for **13** and **14**

Compound	**13**			**14**		
Bond length (Å)	C1–C24	C6–C31	C15–C38	C1–C24	C6–C31	C15–C38
	1.500 (4)	1.507 (5)	1.481 (4)	1.498 (5)	1.497 (5)	1.482 (5)
	{1.505 (5)}	{1.496 (4)}	{1.482 (4)}	{1.509 (5)}	{1.506 (5)}	{1.480 (5)}
Dihedral angle	A	B	C	A^1	B^1	C^1
	56.72°	74.71°	64.89°	62.17°	76.88°	33.39°
	{65.01°}	{64.18°}	{56.72°}	{56.50°}	{54.66°}	{52.34°}

The values in the brackets { } corresponds to second molecule of the asymmetric unit. A is the dihedral angle between 4-methylphenyl ring attached to C1 carbon and expanded corrole plane formed by three *meso*-carbons. B is the dihedral angle between 4-methylphenyl ring attached to C6 carbon and expanded corrole plane formed by three *meso*-carbons. C is the dihedral angle between 4-nitrophenyl ring attached to C15 carbon and mean expanded corrole plane formed by three *meso*-carbons. Similarly A^1, B^1, C^1 are the corresponding dihedral angles for compound **14**.

(H68···O5, 2.731 Å; C68–H68···O5, 132.27°). The other crystallographically independent molecule (shown in green color) forms a head to head dimer with its nearest neighbour involving two C–H···O interactions (shown in cyan color) with oxygen of nitro group and C–H of *meso*-aryl group bearing nitro groups (H42···O3, 2.480 Å; C42–H42···O3, 168.35°). The linear chain formed from the one asymmetric unit and head to head dimer formed from other unit are linked to each other through another C–H···O interaction (shown in orange color) involving the oxygen of the nitro group (same oxygen involved in linear chain formation) with the β C–H of furan ring (H4···O5, 2.406 Å; C4–H4···O5, 142.12°) leading to the supramolecular array.

Table 4
Dipole moments and HRS hyperpolarizabilities at 1064 nm

Compound	μ (Debye)	β (10^{-30} esu)
1	1.20	1.90
2	3.20	7.20
3	4.60	10.1
4	32.0	54.0
12	9.82	30.08
13	9.73	29.67
14	8.66	26.54
15	8.59	24.17
5	–	1501
6	–	4933

3.3. Nonlinear optical properties

The molecular first hyperpolarizability (β) values determined by Hyper–Rayleigh scattering method for compounds **12**–**15** along with their calculated ground state dipole moment are listed in Table 4. For the sake of comparison, the β value and dipole moments for the push–pull porphyrins **1**–**6** measured by HRS method at 1064 nm is also included in the table. Fig. 6 shows linear dependence of HRS intensity on the chromophore number density, indicating that chromophore concentration is in the dilute solution limit.

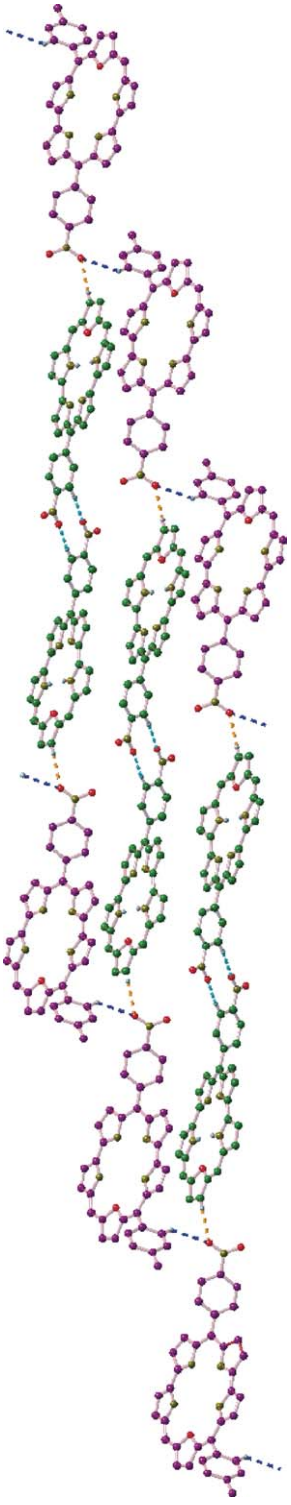

Fig. 5. A view of supramolecular array formed by **13**.The molecules of the asymmetric unit are shown by different color. The secondary interactions are shown by dashed lines.

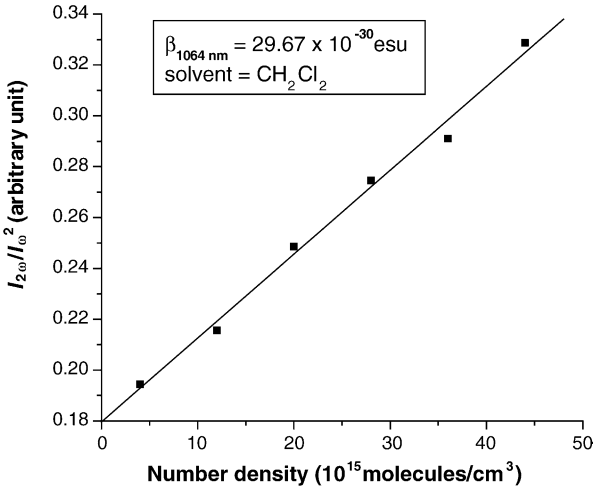

Fig. 6. $I_{2\omega}/I_{\omega}^2$ vs. number density of **13** in CH_2Cl_2. The solid line is best linear fit.

From the slope of plot we extracted hyperpolarizability values after comparison with an external reference. It is clearly seen from the table that the β values for compounds **12**–**15** are roughly 4–5 times larger compared to corresponding, structurally similar tetraphenyl porphyrin derivatives **1** and **2** which have donor-acceptor group present on *meso*-phenyl substituents. This observation clearly suggests that the nonlinear optical response can be enhanced by enhancing the availability of mobile electrons in the porphyrin skeleton, which in turn can play a key role in enhancing the polarization of molecular system (Note that compound 1 and 2 have 18 π electrons while compounds **12**–**15** have 22 π electrons in conjugation). However, it should be mentioned here that the β values observed in the present study are only moderate considering the fact that these macrocycles have more number of π electrons. This decrease in the nonlinear response is attributed to the loss of effective communication between the expanded corrole core and the donor acceptor groups which reduces the effective charge transfer because of large dihedral angle between the macrocycle and *meso*-substituents (Table 4) [17]. It has been predicted that the β value is reduced by 50% if the dihedral angle [18] is around 60°.

The larger value observed for compound **4** is attributed to the presence of electron withdrawing nitro group on the β pyrrole position rather than on the *meso*-phenyl ring. The presence of electron withdrawing group on the β position generally results in only one net charge transfer direction thus enhancing the possibility of nonlinear response [3b]. The very large β value observed for compound **5** and **6** is attributed to the presence of electronic coupling facilitated by the presence

of donor, acceptor, linker and the chromophore in the same plane which is a predominant factor for effective electronic interaction within the molecule [19].

4. Conclusion

Synthesis of four new push–pull expanded corroles is described along with two X-ray structures for the newly synthesized compounds. The first molecular hyperpolarizability β measured show larger values for the 22 π systems relative to structurally similar 18 π porphyrins revealing the fact that nonlinear response can be enhanced by increasing the number of π electrons in conjugation. The search for new materials for NLO application requires optimization of β values with respect to the structure of macrocycle and the orientation of donor and acceptor groups. Recently it has been predicted that substantially larger NLO response is obtained when donor groups are attached to electron rich centre on the porphyrin macrocycle and the electron acceptor group attached to electron deficient centre [20]. In the expanded corroles described here the β pyrrole positions have larger electron density relative to the *meso*-carbons [21]. Thus, substitution of electron donating group on the β pyrrole position could substantially enhance the second order NLO response. Another strategy is to substitute all *meso*-position by electron donor and only one electron withdrawing group in β position to have only one charge transfer direction. Synthesis of such molecules is in progress in this laboratory.

Acknowledgements

This work was supported by grants from the Department of Science and Technology (DST) and Council of Scientific and Industrial Research (CSIR), Government of India, New Delhi. We thank Prof. P.K. Das, IISc, Bangalore for Nonlinear Optical measurements. We thank Dr. Asha for useful discussion. R.M., R.K. and V.P.R. thank CSIR for their fellowships.

References

[1] (a) D.S. Chemla, J. Zyss, Nonlinear Optical Properties of Organic Molecule and Crystals, vols. 1–2, Acadmeic Press, New York, 1987;
(b) P.N. Prasad, D.R. Ulrich, Nonlinear Optical and Electroactive Polymers, Plenum, New York, 1988;
(c) D.R. Kanis, M. Ratnere, T.J. Marks, Chem. Rev. 94 (1994) 95–242.
[2] S.R. Marder, J.W. Peery, Adv. Mater. 5 (1993) 804, and references therein.
[3] (a) K.S. Suslick, C.T. Chen, G.R. Meredith, L.T. Cheng, J. Am. Chem. Soc. 114 (1992) 64928–64930;
(b) A. Sen, P.C. Ray, P.K. Das, V. Krsihnan, J. Phys. Chem. 100 (1996) 1961–19613;
(c) S.M. Lecours, H.W. Guan, S.G. DiMango, C.H. Wang, M.J. Therien, J. Am. Chem. Soc. 118 (1996) 1497–1503;
(d) M. Yeung, A.C.H. Ng, M.G.B. Drew, E. Vorpagel, E.M. Breitung, R.J. McMohan, D.K.P. Ng, J. Org. Chem. 63 (1998) 7143–7150;
(e) J.H. Chou, M.E. Kosal, H.S. Nalwa, N.A. Rakow, K.S. Suslick, in: K.M. Kadish, K.M. Smith, R. Guilard (Eds.), Porphyrin Handbook, vol. VI, Academic Press, San Diego, 1999, pp. 53–58 (Chapter 41).
[4] S. Venkatraman, R. Kumar, J. Sankar, TK. Chandrashekar, K. Sendhil, C. Vijyan, A. Kelling, MO. Senge, Chem. Eur. J. 10 (2004) 1423–1432.
[5] (a) G.M. Sheldrick, SHELXS-93f, Universitat Gottingen, 1993;
(b) G.M. Sheldrick, SHELXL-97, Universitat Gottingen, 1997.
[6] T. Kodaira, A. Watanabe, O. Ito, M. Matsuda, K. Clays, A. Persoons, J. Chem. Soc., Faraday Trans. 93 (1997) 3039–3044.
[7] P.C. Ray, P.K. Das, J. Phys. Chem. 99 (1995) 14414–14417.
[8] B. Sridevi, S.J. Narayan, A. Srinivasan, M.V. Reddy, T.K. Chandrashekar, J. Porphyrins Phthalocyanines 2 (1998) 69–78.
[9] A. Srinivasan, B. Sridevi, M.V. Reddy, S.J. Narayan, T.K. Chandrashekar, Tetrahedron Lett. 38 (1997) 4149–4152.
[10] S.J. Narayan, B. Sridevi, T.K. Chandrashekar, A. Vij, R. Roy, J. Am. Chem. Soc. 121 (1999) 9053–9068.
[11] S. Venkatraman, T.K. Chandrashekar, Acc. Chem. Res. 36 (2003) 676–691.
[12] S. Dahal, V. Krishnan, J. Photochem. Photobiol. A: Chem. 89 (1995) 105–112.
[13] B. Sridevi, S.J. Narayanan, T.K. Chandrashekar, U. Englich, K. Ruhlandt-Senge, Chem. Eur. J. 6 (2000) 2554–2563.
[14] J.R. Lakowicz, Principles of Fluorescence Spectroscopy, second ed., Kluwer Academic, Plenum Publishers, New york, 1999, p. 11.
[15] (a) Y.H. Kim, H.S. Chao, D. Kim, S.K. Kim, N. Yoshida, A. Osuka, Synth. Met. 117 (2001) 183–187;
(b) H.N. Fonda, J.V. Gilbert, R.A. Comier, J.R. Sprague, K. Kamioka, J.S. Connolly, J. Phy. Chem. 97 (1993) 7024–7033.
[16] Sapphyrin is a molecule having five pyrrole and four meso-carbons.
[17] G.D.L. Torre, P. Vazquez, F.A. Lopez, T. Torres, Chem. Rev. 104 (2004) 3723–3750.
[18] P.C. Leung, J. Stevens, R.E. Harelstad, M.S. Spiering, D.J. Gerbi, C.V. Francis, J.E. Trand, G.V.D. Tiers, G.T. Boyd, D.A. Ender, R.C. Williams, Proc. SPIE-Int. Soc. Opt. Eng. 1147 (1989) 48–60.
[19] I.D.L. Albert, T.J. Marks, M.A. Ratner, Chem. Mater. 10 (1998) 753–762.
[20] (a) P.R. Varanasi, A.K.Y. Jen, J. Chandrasekhar, I.N.N. Namboothri, A. Rathna, J. Am. Chem. Soc. 118 (1996) 12443–12448;
(b) I.D.L. Albert, T.J. Marks, M.A. Ratner, J. Am. Chem. Soc. 119 (1997) 6575–6582.
[21] M. Gouterman, in: D. Dolphin (Ed.), The Porphyrins, vol. 3, Academic, New York, 1978 (Chapter 1).